# Optimal design, manufacturing and testing of non-conventional laminates

Peeters, Daniël M.J.; Irisarri, François Xavier; Groenendijk, Chris; Růžek, Roman

**DOI**
10.1016/j.compstruct.2018.10.062

**Publication date**
2019

**Document Version**
Accepted author manuscript

**Published in**
Composite Structures

# Optimal design, manufacturing and testing of non-conventional laminates

Daniël M.J. Peeters*[a], François-Xavier Irisarri[b], Chris Groenendijk[c], Roman Růžek[d]

[a]*Delft University of Technology, faculty of aerospace engineering*
[b]*DMAS, ONERA, Université Paris Saclay, F-92322 Châtillon, France*
[c]*Dutch Aerospace research centre (NLR)*
[d]*VZLU - Czech Aerospace Research Centre, Strength of Structures Department, Beranových*

**Abstract**

Composite materials are finding increasing application, for example in commercial aircraft. Traditionally fiber angles are restricted to 0°, ±45° and 90°. The current work exploits the possibility of using multiple 'non-conventional' laminates where either fiber steering ('variable stiffness'), ply drops ('variable thickness'), or a combination of both is used. This leads to varying mechanical properties which means the load is being redistributed, increasing the overall buckling load. A flat panel of $400 \times 600$ mm loaded in uni-axial compression is optimized in the current work. As a benchmark a conventional laminate is used. The non-conventional laminates are 15% lighter to emphasize the possible weight savings. Only using variable stiffness or variable thickness is experimentally shown to not be sufficient to match the buckling load of the benchmark panel. However, using a combination of both, a 10% increase in the buckling load was found for a panel that is 15% lighter. This highlights the potential of non-conventional laminates.

*Keywords:* Variable Stiffness; Fibre Steering; Fibre Placement; Testing; Variable Thickness

## 1. Introduction

Today, composite materials are finding increasing application in large commercial aircraft and the first composite-dominated planes like the B-787 or A350 are being built. Traditionally, fibers within a layer have the same orientation, leading to constant stiffness properties. As manufacturing

*Currently post-doc at University of Limerick, school of engineering, Bernal Institute
*Email address:* daniel.peeters@ul.ie (Daniël M.J. Peeters )

technology has evolved, for example with the advent of automated fiber placement machines, the fiber orientation of a layer can be varied continuously leading to varying stiffness properties that can be best tailored for the applied loads. These composites are called variable stiffness laminates (VSL) in the current work.

One of the largest problems in optimizing VSL is taking manufacturability into account. To do this, linearly varying fibre angles are used by many researchers which have given promising, manufacturable, results [1, 2, 3, 4, 5, 6]. The use of linearly varying fiber angle per bay, for stiffened plates, has also been investigated, and again it has been shown that varying the fiber angles leads to better performance [7, 8]. Direct parametrisation of the tow paths using Lagrangian polynomials [9, 10, 11] Lobatto-Legendre polynomials [12, 13], Bezier curves [14, 15, 16], splines [17, 18], B-splines surfaces [19] and NURBS (Non-Uniform Rational B-Splines) [20] have also been used. Constant curvature paths have been extensively applied for flat panels and for cylindrical and conical shells [21, 22, 23, 24, 25], as the curvature constraint evaluation is simplified. Large, manufacturable, improvements in buckling load were found, but the result is dependent of the basis functions chosen [20, 26, 9]. Hence, the total potential of VSL has not been exploited due to the pre-specified set of possibilities. Furthermore, most methods assume that the fibers are shifted, meaning a choice has to be made whether gaps or overlaps are allowed during manufacturing [27]. For instance, gaps and overlaps are observed in the cylindrical shells manufactured by Wu et al. [21] and the flat plates manufactured by Tatting and Gürdal [28].

Another approach that leads to manufacturable designs is to align the fibres in the direction of principal stress. This has been shown to reduce stress concentrations, and can also lead to reduced weight using the tailored fiber placement method [29, 30]. Using load paths, or a hybrid combination of load paths and principal stress direction has also been used to design VSLs [31]. Continuous tow shearing is a new manufacturing method, leading to varying fiber angles without any gaps or overlaps, but with a thickness variation that is coupled with the change in fiber angle [32, 16]. By using a genetic algorithm, coupled with a pattern-search algorithm, or using the infinite strip method, large improvements in structural performance have been shown [33, 34]. A more comprehensive review of optimization strategies can be found in Ghiasi et al. [35]

To exploit the possibilities of VSL fully, a three-step approach has been developed at Delft

University of Technology. The first step is to find the optimal stiffness distribution in terms of the lamination parameters. This is discussed in detail in IJsselmuiden [36, 37]. The second step is to find the optimal manufacturable fibre angle distribution [38, 39, 40]. The third step is to retrieve the fiber paths, discussed in Blom [41]. A schematic overview of this approach is shown in Figure 1.

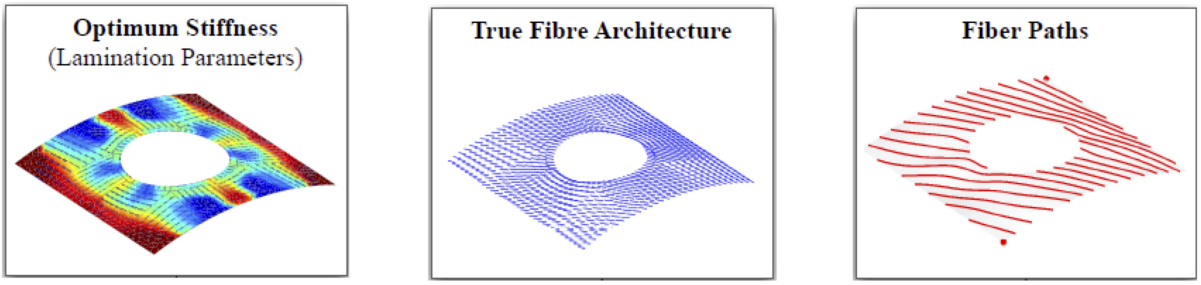


**Figure 1. schematic overview of the three-step optimization approach [36]**

Another way to achieve varying mechanical properties is by changing the thickness over the structure, leading to variable thickness (VT) structures. Thickness variation in a laminate is described using two variables: the ply drop location and the ply drop order. The most popular approach is to use an evolutionary algorithm, typically a genetic algorithm, to optimize the number of layers per 'patch', while also optimizing the ply drop order and stacking sequence, limited to a discrete set of angles (e.g., 0°, ±45°, and 90°). This area of research is referred to as laminate blending [42, 43, 44, 45, 46] and assumes that potential ply drop locations (i.e., patch boundaries) are pre-specified by the user. A technique where the fiber angle is not restricted to a discrete set has also been developed, however, no manufacturing constraints, limiting the change in fiber angle from one element to the next, are posed [47].

Other techniques where the ply drop locations are not pre-specified use continuous optimization. Shape optimization [48] is used to determine the shape and hence ply coverage and ply drop locations of the different layers. The optimization is performed using a level-set approach with fiber angles limited to a discrete set. Another continuous method is the discrete material and thickness optimization method, where the fiber angles belong to a discrete set and fictitious density

variables are used to select the ply angles at any given location. This has been done for compliance and buckling optimization [49, 50]. For this method, also a thickness filter has been implemented to get to physically feasible designs [51]. Thickness optimization for buckling load under uni- and bi-axial compression has also been performed. This work showed that large improvement in buckling load could be made without affecting the in-plane stiffness[52].

The easiest ply drop orders are inner or outer blending, where the layers are dropped from the symmetry plane, or from the outside respectively. To determine the optimal ply drop order, guide-based designs can be used: [43] a stacking sequence for the thickest laminate, called the guide laminate, is defined and the number of layers per patch. The stacking sequence is then derived by dropping layers from the inside or outside, depending whether inner or outer blending is used, from the guide laminate. A method that offers more possible ply drop orders and takes into account industrial guidelines is using stacking sequence tables [53]. A ply drop order and guide laminate are optimized. The outer layer is most often not dropped since this would create a defect on the outside, from where cracks or a delamination could start.

One of the first variable stiffness plates was manufactured and tested by Hyer et al. [54], based on optimized designs that were adapted to allow manufacturing [55]. The fiber paths were chosen to go around the cut-out as can be seen in Figure 2. These fiber paths preserved continuity of the fibers going around the cut-out, trying to lead the load away from the cut-out. During testing, it was found that the buckling load increased. However, since the paths at the side were not continuous, the tensile strength was reduced: fiber continuity of these fibers was not preserved. Hence, the idea of leading the load away was shown to work in practice, but due to manufacturing reasons, the tensile strength decreased.

When manufacturing panels with linearly varying fiber angles, a choice has to be made whether gaps or overlaps are allowed when shifting the tows: either gaps or overlaps appear, or the width of the tow has to be changed, as shown in Figure 3. Both options were manufactured, and as a reference, a constant stiffness laminate (CSL) was manufactured. All three types of panels were tested for buckling under compression and shear load [56, 57]. Under compression, the buckling load of the CSL was predicted quite accurately: the buckling load of panels with gaps was on average about 10% higher than predicted, the buckling load of the panels with overlaps was almost

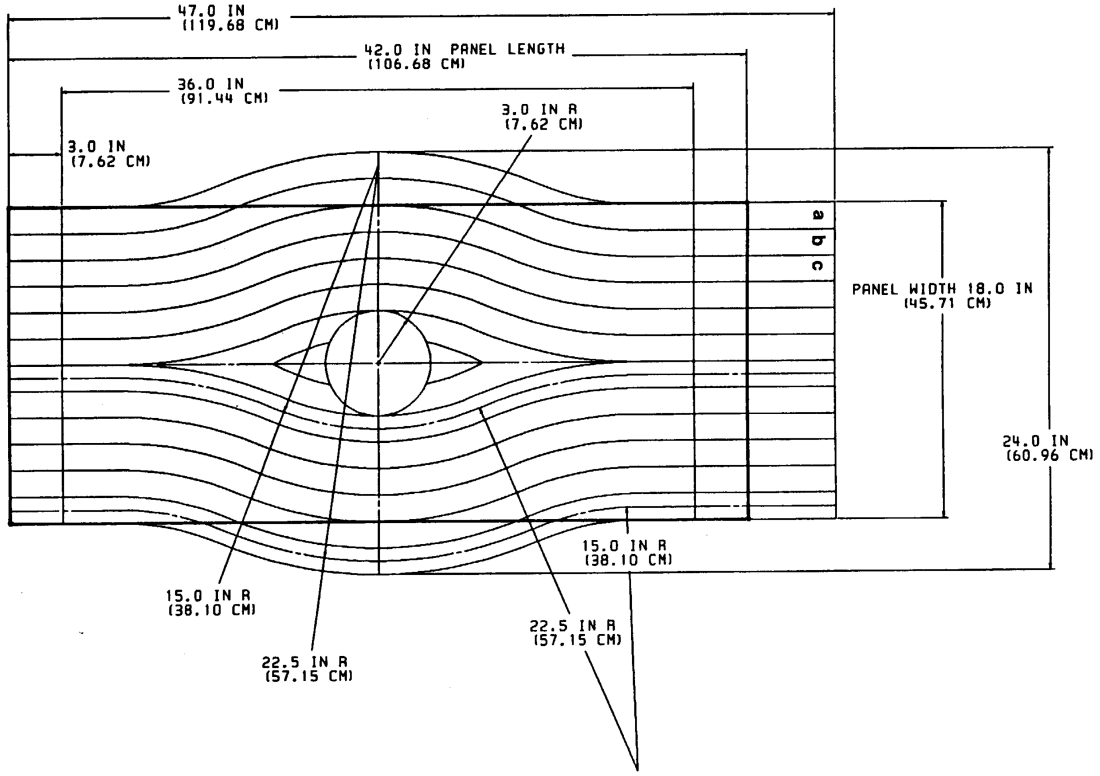


**Figure 2. Steered paths manufactured by Hyer et al. [54].**

50% higher than the predicted load. This is the result of a combination of effects: due to curing some pre-stress appears, which has a positive effect on the buckling load. Furthermore, the actual material properties could differ from the assumed properties, and the gaps and overlaps have not been taken into account [56]. The buckling results under shear load were different: the buckling load was predicted accurately for both the panel with gaps and overlaps. The buckling load of the VS panels under shear is lower than that of the CS panels, because they were optimized for buckling under compression. The failure load on the other hand is increasing [57]. These tests clearly show that VSLs lead to an actual increase in performance, not just to a theoretical one.

Some VSL cylinders have been built and both a modal and bending test was performed [58]. The results for both the modal and bending tests showed good agreement between FEA and experiments, for both mode shape and modal frequency, as well as for the strain field. It was noted

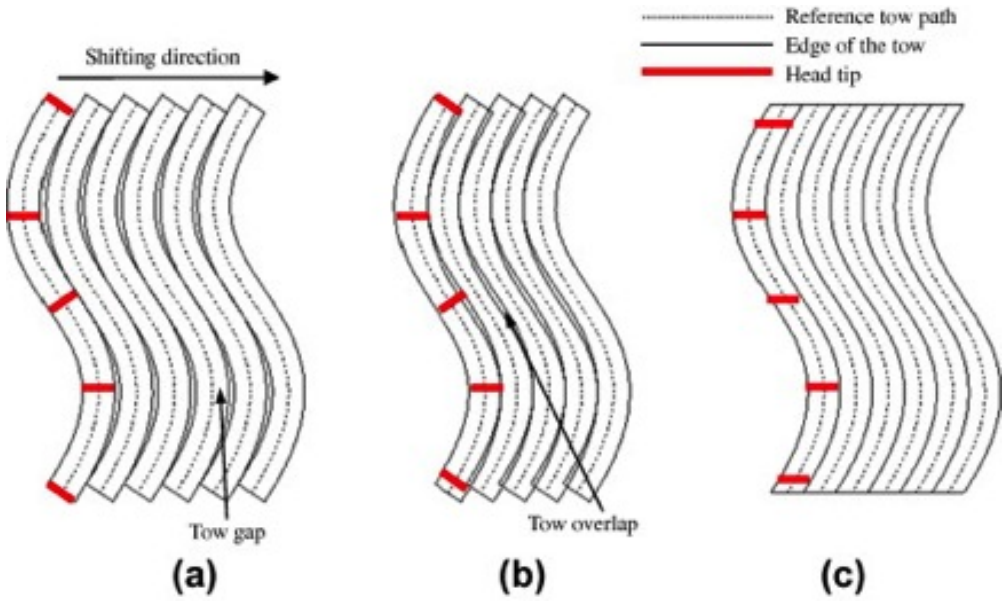


**Figure 3. Gaps and overlaps appearing when shifting [16].**

that the load redistribution behaves as expected: the tension side carried a larger part of the load than the compressive side. Furthermore, the maximum strain at the same load was significantly reduced: the compressive strain was 10% lower, the tensile strain even 35% compared to the CSL design. This shows the potential when a strength-critical design is optimized using VSL: using a strain-based failure criterion, this reduction in strain is significant. Hence, these tests again confirmed the possibilities to improve structural performance by using VSLs.

Another set of cylinders was built and a series of tests was done by Wu in cooperation with different co-workers. The same VS cylinders were used for a series of tests [59, 60]: first pristine (i.e, as manufactured without any cut-outs) [61], then making cut-outs in them [62], followed by large cut-outs [63]. Two cylinders were manufactured and tested with the same fiber angle distribution. The only difference is that one cylinder is manufactured using an overlap strategy, the other using the gap strategy. The difference in weight, for the pristine cylinders, is 27%. The axial stiffness and buckling load, normalized with respect to the weight, is 28% and 78% higher for the cylinders made using the overlap strategy compared to the cylinders made using the gap-strategy respectively. The experiments agree within 10% with FEA, suggesting that VS cylinders are less sensitive to imperfections than their CS counterparts [61].

The cylinders were not damaged during the buckling test, and another set of tests was done, with a cut-out on one side scaled to represent a passenger door on a commercial aircraft [62]. Even though the cylinders were not designed to have a cut-out, the decrease in mechanical performance compared to the pristine (i.e., without cut-out) cylinder was not large: on average 93% (94 and 91% was measured) of axial stiffness, and 86% (82 and 91% was measured) of buckling load remains compared to the pristine cylinders. This shows the advantage that VS cylinders offer: the influence of cut-outs is small. Furthermore, it is expected that this influence could be further reduced when they are accounted for during design [62]. It has to be noted that the cut-outs were made in the low-stiffness part of the cylinder, which could be part of the reason for the small influence.

The cylinders still did not show any sign of damage, so the size of the cut-out was increased to represent a cargo door on a commercial aircraft. Increasing the size of the cut-out had a limited effect on the performance: on average still 91% (92% and 90% was measured) of axial stiffness and 85% (both 85%) of buckling load was preserved compared to the pristine cylinders. For the tests with cut-outs good agreement was found with the linear bifurcation buckling loads. Since it is known that the buckling load of unstiffened CS cylinders and plates are sensitive to geometric imperfection recently, a numerical study on the influence of imperfections on the performance of VS cylinders has been performed [64]. Results showed what was expected based on the previous results: the imperfections have a limited influence. The reason is that the buckling always occurs in the same region: by varying the fibre angle a large difference in local stiffness is created. Hence, the location of the buckling is not influenced by imperfections. This implies that the load redistribution is hardly influenced by the imperfections, and thus the effect of these imperfections is small [64].

Recently a thermoplastic VS wingbox was designed, manufactured and tested at the University of Limerick. This was a unified approach: the stiffeners and skin were connected in-situ without the need for secondary processes. No CS counterpart was made, but finite element analyses showed a 14% improvement in buckling load. The experimentally obtained buckling load matched the predictions very well [65, 66].

In this paper three different manufacturing approaches are compared: variable stiffness, vari-

able thickness and a combination of both. As a reference a CS laminate is made and tested. The VS, VT, and VSVT laminates are 15% lighter than the CS laminate. The problem formulation and optimization is discussed in section 2. Next, the changes necessary for manufacturing and the manufacturing itself are discussed in section 3. The tests are described in section 4. A detailed discussion is provided in section 5. Finally, the paper is concludes with section 6.

# 2. Optimization

## 2.1. Overview of the optimization method

The optimization performed in the present work is a direct application of the optimization strategy previously published in [67]. The strategy combines fiber steering optimization [68, 37], ply drop location [69] and ply drop order optimization using stacking sequence tables (SSTs) [70]. The approach fits into the three-step optimization framework proposed by IJsselmuiden for VSLs and mentioned in the introduction of this paper (see Figure 1). First, a structural optimization is performed using a homogenized representation of the laminates based on lamination parameters. The output is an idealized design defined by a thickness distribution and stiffness distribution over the structure. Second, the optimal fiber angle and ply-by-ply material distributions are retrieved. In [67], the second optimization step is divided into two successive optimization phases, referred to as Step 2.1 and Step 2.2 respectively. Both phases combine an evolutionary optimizer, for its efficiency in solving combinatorial problems and escaping local optima, and a gradient-based optimizer, for its efficiency in handling numerous design variables and constraints in continuous problems. A schematic overview is shown in Figure 4

Step 2.1, starts by a SST evolutionary optimization that aims at providing an initial set of variable-thickness straight-fiber designs closely matching the thickness and stiffness distributions of the idealized design issued from the first optimization step. The evolutionary algorithm (EA) performs a Pareto optimization with two objectives to minimize: an estimate of the distance to the target stiffness distribution in membrane and its counterpart in terms of bending stiffness. Each solution is defined by a guide laminate, a ply drop order and a distribution of ply numbers. The

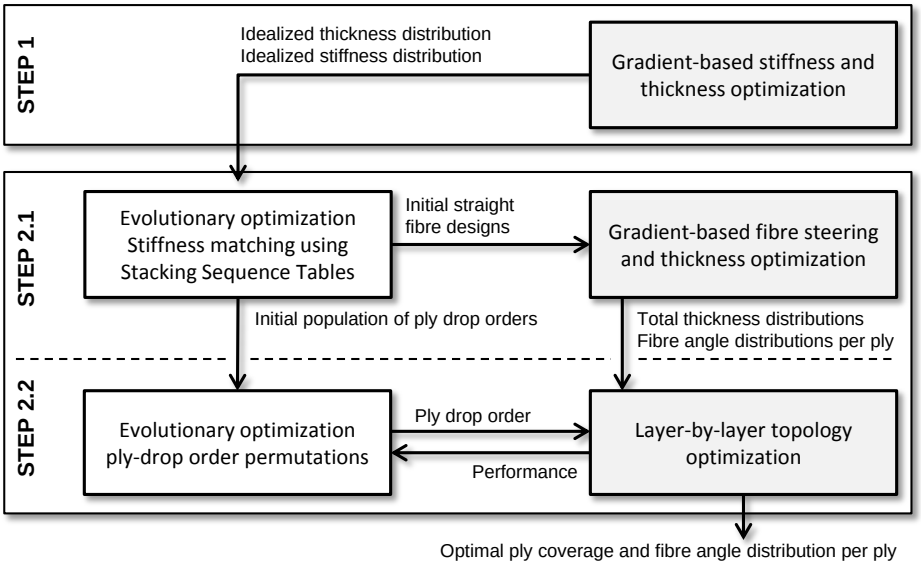


**Figure 4. Schematic overview of the optimization strategy.**

obtained non-dominated solutions are subsequently improved using gradient-based optimization with respect to the objective and constraints of the first step structural optimization. Starting from the ply-per-ply constant fiber orientation and the ply number distribution returned by the EA, the optimizer returns ply-per-ply fiber orientation distributions, corresponding to steered plies, and a thickness continuous distribution over the structure. The ply-drop order is fixed, however the optimization result depends on it since it is assumed that all plies likely to be dropped share the same thickness reduction at each point of the structure whereas plies that cannot be dropped keep their initial thickness that corresponds to the thickness of the base ply material. Consequently, the optimization has to be repeated for all combinations of plies that cannot be dropped. In the current work, it is assumed that the outer ply cannot be dropped. The outcome of Step 2.1 is a set of candidate designs with optimal thickness distribution and fiber angle distributions. However the ply drop locations are still not known.

Retrieval of the ply drop locations based on the thickness continuous distribution is performed in Step 2.2. Evolutionary optimization and topology-like gradient-based optimization are closely intertwined. A permutation evolutionary algorithm is used to optimize the ply-drop order within the laminate. Each solution evaluation calls for a continuous optimization of the ply-drop location.

Topology-like optimization is performed using a fictitious density distribution for each ply, under a volume constraint. At each point of the structure, the density of a ply is constrained with respect to the density of all other plies to comply with the imposed ply-drop order. Plies that cannot be dropped are fixed just like in Step 2.1. In all other plies, the densities are forced to converge to either zero or one, thus defining a clear topology for each ply. The gradient-based optimizer alternates between ply-per-ply density optimization and updates of the fiber angle distribution in each ply. The outcome of Step 2.2 is a steered VSVT laminate with optimized fiber angle distribution and optimal ply-drop location in each ply. The overall strategy allows to handle both symmetry and balanced design guidelines as well as a steering constraint that tends to minimize the number of gaps and overlaps at global level and ensures a minimal curvature radius for the tows at local level.

## 2.2. Buckling maximization for rectangular panels under compression

The optimization strategy has been applied to the buckling maximization of rectangular panels under compression. The panels are assumed to be simply supported on their four edges and the loaded sides are considered to remain straight. The panel dimensions are $600 \times 400$ mm. Uniaxial compression is applied in the direction of the length of the panel, which also corresponds to the $0^\circ$ direction in the following. Two materials have been benchmarked in this study: Cytec PRISM TX1100 with EP2400 PRISM resin and Hexcel HiTape material with RTM6 resin. The material in-plane orthotropic elastic properties have been assumed to be the same for both materials with $E_{11}$ = 154 GPa, $E_{22}$ = 10.8 GPa, $G_{12}$ = 4.02 GPa and $\nu_{12}$ = 0.317. The ply thickness is 0.19 mm for the TW1100, while for the HiTape the thickness is 0.12 mm. Thus 40 layers of HiTape or 26 layers of TX1100 give the same total thickness of 4.94 mm.

Manufacturing tests using the AFP machine at NLR showed that the minimal turning radius required to avoid wrinkling is about 800 mm for the TX1100 and 400 mm for the HiTape. Two benchmarks have been defined, one for each material. A CS laminate and a VT straight-fiber laminate have been manufactured using TX1100 material. A CS laminate, a VS laminate without any ply drop and a VSVT laminate have been manufactured using HiTape material since the smaller

steering radius gives a larger improvement in the buckling load. Since the current industry standard often limits the possible fiber angles to 0°, ±45°, and 90°, the benchmarks only consist of these angles. For the best buckling performance, a lot of ±45° plies are wanted, and it is best practice to put them next to each other. As a constraint on the compliance is imposed during the optimization, this constraint is posed to the benchmarks as well. Hence, some 0° plies are added: 6 for the HiTape material and 4 for the TX1100 were found to be necessary. To satisfy the 10% rule also a 90° ply has to be included. As a final constraint, no 0° and 90° ply should be put next to each other. The lay-up chosen for the TX1100 CS laminate is [45 -45 0 0 45 -45 90 45 -45 0 45 -45 0]$_s$ while the lay-up chosen for the HiTape CS laminate is [45 -45 0 0 45 -45 90 90 45 -45 0 0 45 -45 0 0 45 -45 90 90]$_s$. The expected buckling loads are 71.8 kN and 71.1 kN respectively. Both reference CS designs are very close together such that all designs can be compared to each other.

For the VT, VS and VSVT laminates, the design objective is to save 15% of weight with respect to the reference CS laminates. Thus, by having the VS, VT and VSVT panels of the same weight, the results can easily be compared to each other. Hence, the VS laminate has been designed with 34 plies. For the VT and VSVT laminates, the volume constraint has been chosen such that the weight is 15% lower than the reference panels. All three laminate configurations have been optimized for buckling. They all share the following design constraints. The global in-plane stiffness of the panel has to be at least the stiffness of the "black aluminum" constant thickness laminate with the same weight. In this paper, the "black aluminum" reference laminate is a quasi-isotropic design defined as all lamination parameters equal to zero, hence no stacking sequence is associated with it. The outer plies on the surfaces of the laminate and the inner plies on each side of the mid-plane of the laminate cannot be dropped. All laminates are symmetrical. Balance is imposed by stacking +$\theta$ and -$\theta$-plies together.

The VT panel has been designed with a volume equal to 85% of volume of the 26-ply reference CS panel. The minimum and maximum numbers of plies have been set to 12 plies and 28 plies respectively. The buckling load estimated using a FE linear eigenvalue extraction analysis is 85.2 kN. It is remarkable that even though 15% of weight is saved, the buckling load seems to improve with respect to the reference CS panel. The solution is detailed per pairs of $\pm\theta$-plies in Figure

5. Plies 1 to 14 are detailed only, with ply 1 being the outer ply and ply 14 the inner ply at the symmetry plane. Note that although this panel satisfies the global stiffness constraint, it does not satisfy the 10% design guideline, neither in its original form (at least 10% of plies oriented at $0^\circ$ , $\pm 45^\circ$, and $90^\circ$ everywhere in the panel) nor in its lamination parameter reformulation [71], since the thinnest part of the panel is a pure $\pm 45^o$-laminate. This means that the optimization had a bit more freedom when compared to the VS or VSVT laminate since it does not need to satisfy the 10% rule at every point.

The VS laminate consists of 34 plies. In order to enforce balance, the orientation of the ply at the midplane is set to $90^\circ$. After optimization, the obtained maximum buckling load is 60.2 kN, which corresponds to 15% decrease, while purely based on thickness one would expect a 38% decrease, since buckling scales with the thickness cubed. Plies 1 to 17 are detailed per pairs of $\pm\theta$-plies in Figure 6. Ply 1 is the outer ply. The panel satisfies the 10% design guideline everywhere in the panel.

Finally, the VSVT panel has been optimized with a volume constraint equivalent to a constant thickness 34-ply panel. The minimum and maximum numbers of plies have been set to 20 plies and 44 plies respectively. The higher number of plies is due to the lower ply thickness in this case. The inner plies close to the symmetry plane (the plies numbered 17 to 22) have been fixed to $0^\circ_2$ , $\pm 45^\circ$ , and $90^\circ_2$ to satisfy the 10% design guideline. The expected buckling load is 73.3 kN, slightly over the reference CS panel. Plies 1 to 22 are detailed per pairs of $\pm\theta$-plies in Figure 7. The solid grey parts are the parts of the layer that have been dropped.

# 3. Manufacturing

Even though manufacturing constraints were taken into account during the optimization, some changes were necessary before the manufacturing could be done. The first is changing the fiber paths into splines that can be used as input for the Coriolis machine used to lay down the dry fiber tows. Next, the splines had to be extended to a $500 \times 700$ mm panel since the edges of the panel had to be cut off. Then, the splines were divided in even and odd plies for mirrored and non-mirrored plies. Parallel splines were added since the machine can lay down multiple

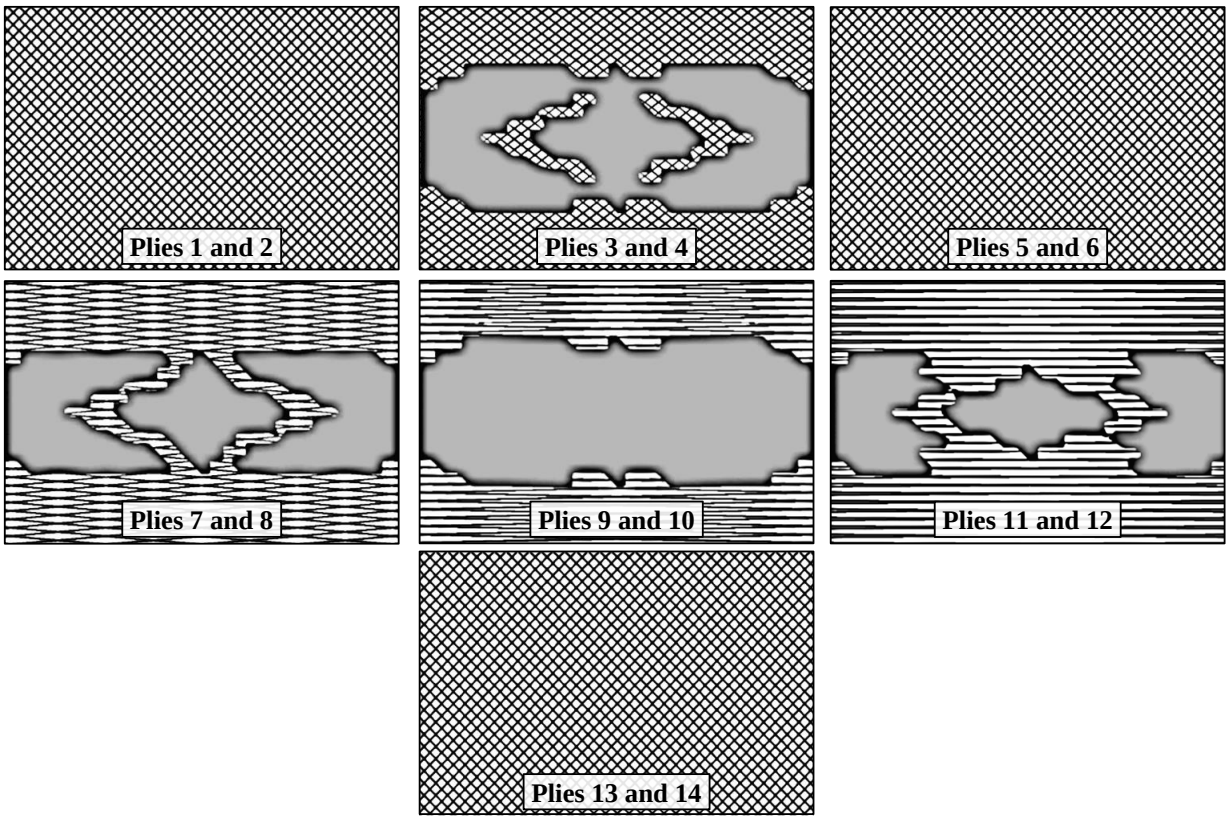


**Figure 5. Straight fiber paths and ply coverage designed for the VT panel. The upper half of the laminate is detailed per balanced pairs of $\pm\theta$-plies. Areas where the plies are dropped are painted in grey color.**

tows in one go. The layers were divided into sectors, with each sector having its own parallel splines. Finally the splines and guidelines for each sector were defined. An example of the start (optimization result) and end point (ready to manufacture) is shown in Figure 8. The VT panels were also slightly changed. To allow for minimum cut length and ease the manufacturing process, the shapes were slightly modified. However, since the minimum cut length and the chosen shapes are machine and user-dependent, this process is not described in detail.

Another important decision is whether gaps or overlaps are generated: due to the fiber steering it is not possible to generate complete plies without gaps or overlaps. In this work, both gaps and overlaps were allowed, with equal importance, a so-called 50% overlap. A graphical representation is shown in Figure 9. This implies that neither gaps or overlaps will be very large, but both

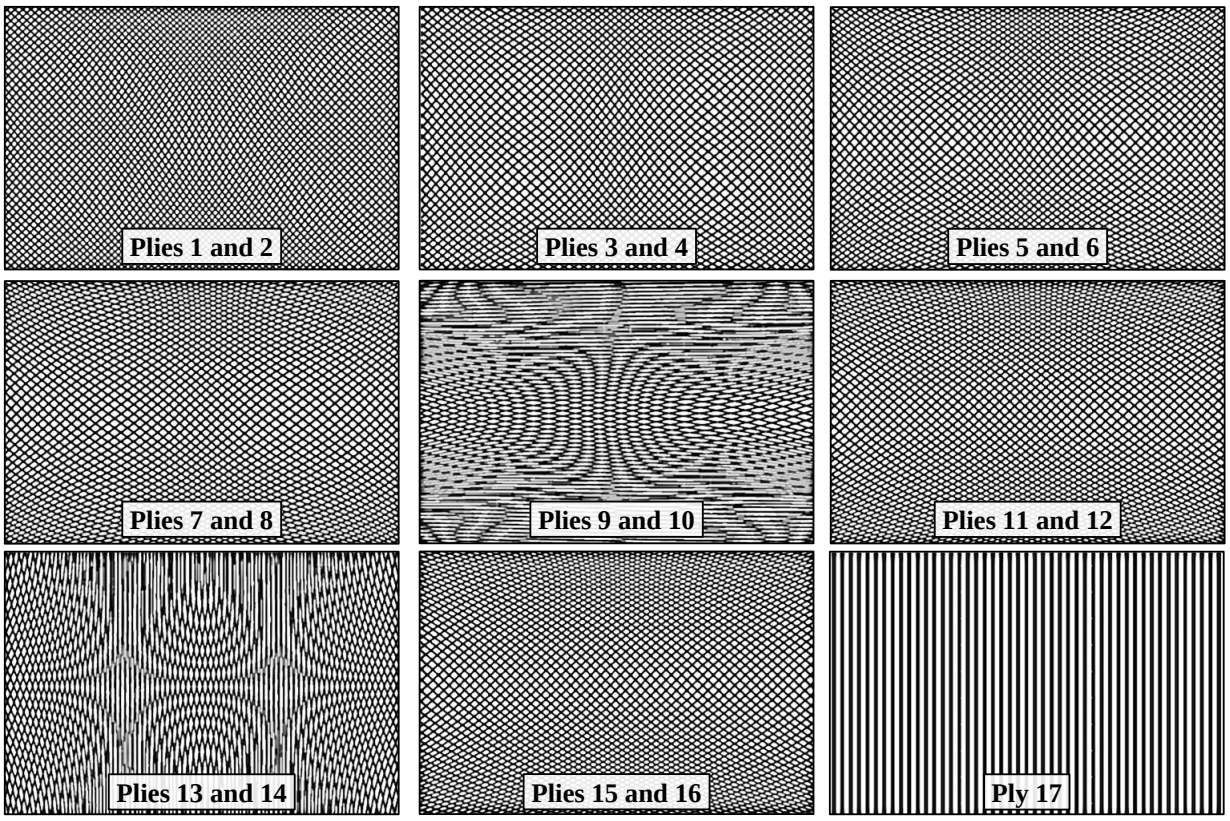


**Figure 6. Steered fiber paths designed for the VS panel. The upper half of the laminate is detailed per balanced pairs of $\pm\theta$-plies.**

exist. A further implication is that the weight of the panels will be close to the weight expected: if only gaps were allowed the panel would be lighter than expected, if only overlaps were allowed, the panel would be heavier than expected.

The tapes that are cut pose another challenge. The moment a tape is cut, it is no longer possible to steer it. Hence, it was tried to avoid internal drops by starting a tape in the panel rather than ending it. However, this was not always possible: some tracks start and end in the panel, meaning one end could not be steered. A single layer manufactured is shown in Figure 10.

NLR infused the dry fiber placed preforms using vacuum infusion (VARTM). All panels were inspected using C-scan immersion approach. No defects were observed and the machined edges were inspected visually. It should be noted that for the VS panel due to the steering the panel surface at the vacuum bag side was quite uneven and through the thickness resin rich zones were

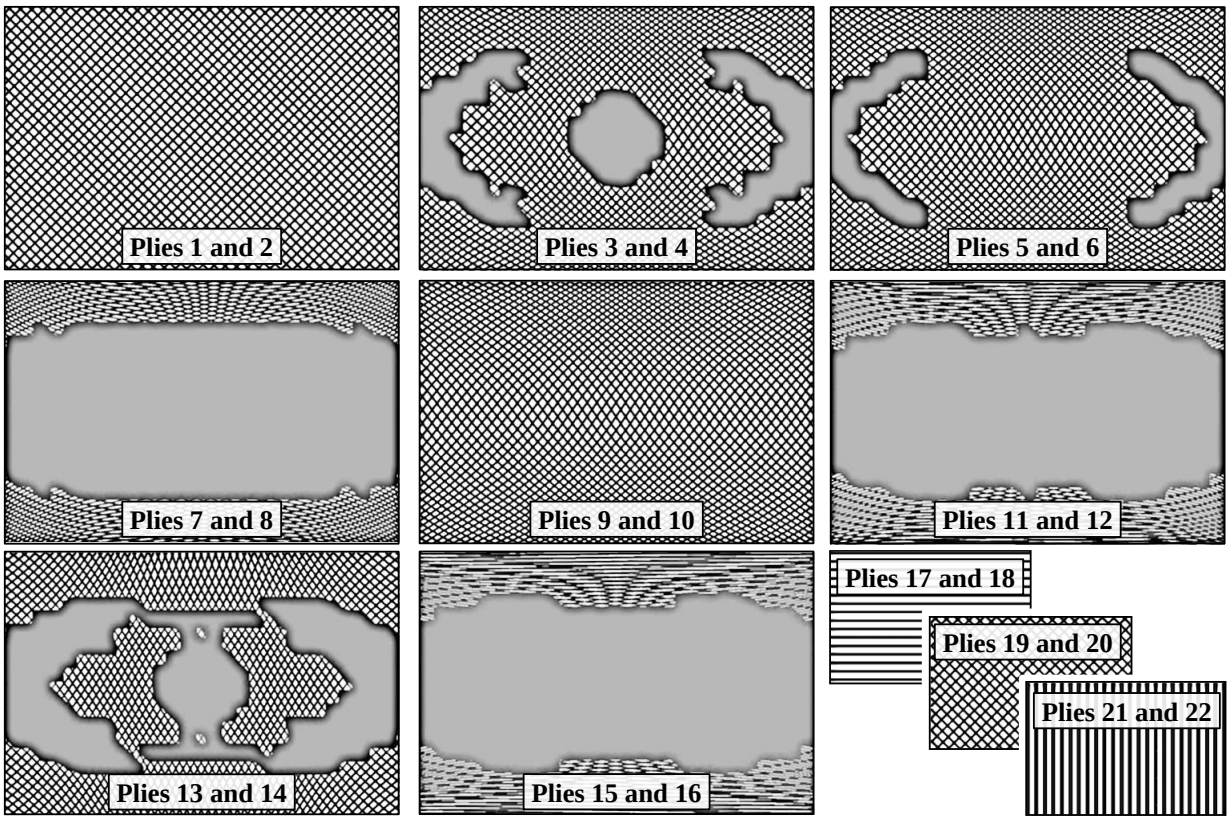


**Figure 7. Steered fiber paths and ply coverage designed for the VSVT panel. The upper half of the laminate is detailed per balanced pairs of $\pm\theta$-plies. Areas where the plies are dropped are painted in grey color.**

observed which make it more complex to interpret the laminate quality using NDI C-scan approach. An example of the completed panels are shown in Figures 11 to 13. For each design, two panels were manufactured. It can be observed in Figure 13 that for the sake of simplicity the variable thickness laminates were manufactured with a flat side. Thus the laminate midplane is not flat as it was assumed in the analysis model.

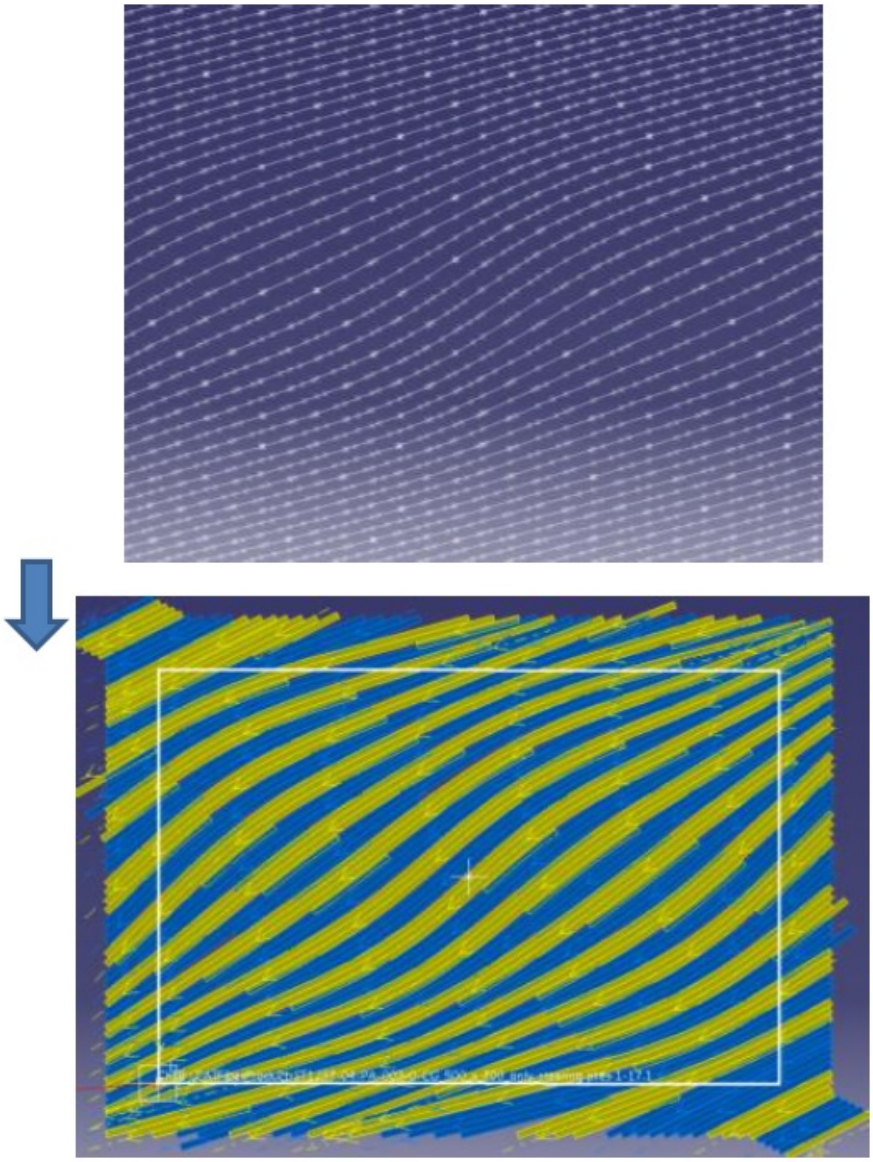

**Figure 8. Result from the optimization (top) and ready to manufacture (bottom) of layer 7 of the VS panel.**

# 4. Tests

## 4.1. Test set-up and data acquisition systems

The test panel arrangement in the test machine is shown in Figure 14. The tests were conducted using the MTS four column load frame system 311.31, with a load capacity of 1000 kN, equipped

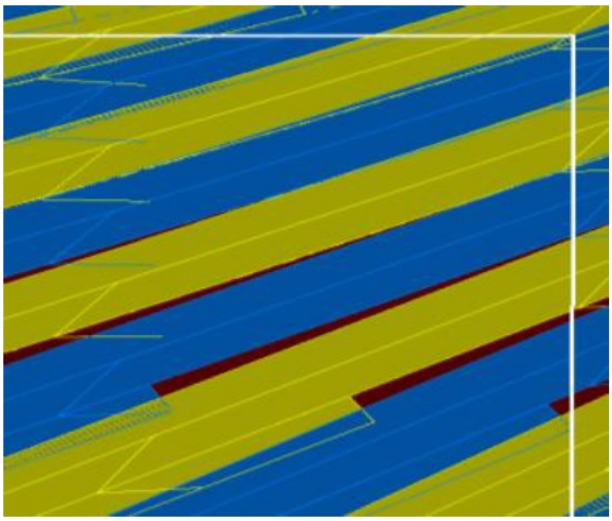

**Figure 9. Close-up of layer 7, showing the 50% gap and overlap.**

**Figure 10. Layer 7, manufactured.**

with a cross head mounted actuator. The panels were tested using vertical guide rails, a bottom support (rail) and a top clamp. The loading conditions were controlled using the MTS FlexTest40 control system [72]. Two back-to-back positioned strain gauges were installed at reference points to check strains in the panel. Strains and deformations were measured using Vishay CEA-06-250UR-350 strain gauges. Data from the Strain gauges were logged, stored and evaluated using the BMCM acquisition system [73] and the NextView 4.2 data acquisition software [74] enabling a real-time data presentation. Additionally, full field deformation measurements of each panel using

**Figure 11. Variable stiffness panel (VS).**

**Figure 12. Variable thickness panel (VT).**

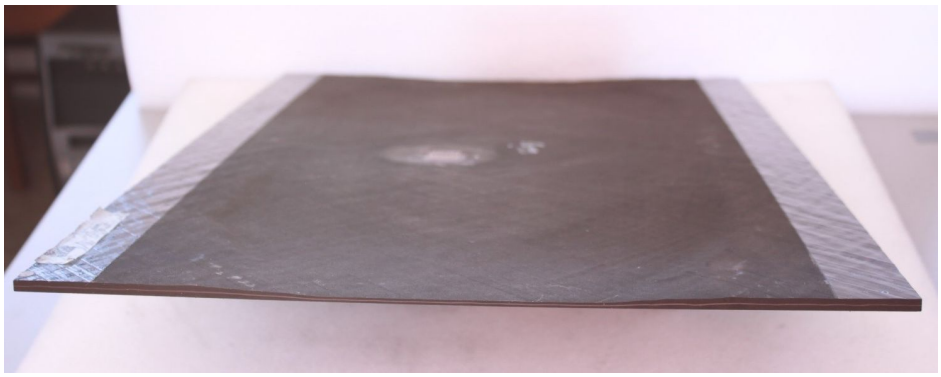

**Figure 13. Variable stiffness variable thickness panel (VSVT).**

a digital image correlation system (DIC) was present to record the out-of-plane displacements. A Dantec Q-400 optical contactless full field measurement system was used for the strain and deformation measurements. The Dantec Q-400 was controlled using the ISTRA 4D software

package [75]. An overview of the test frame with the test panel and Dantec Q-400 camera is shown in Figure 15.

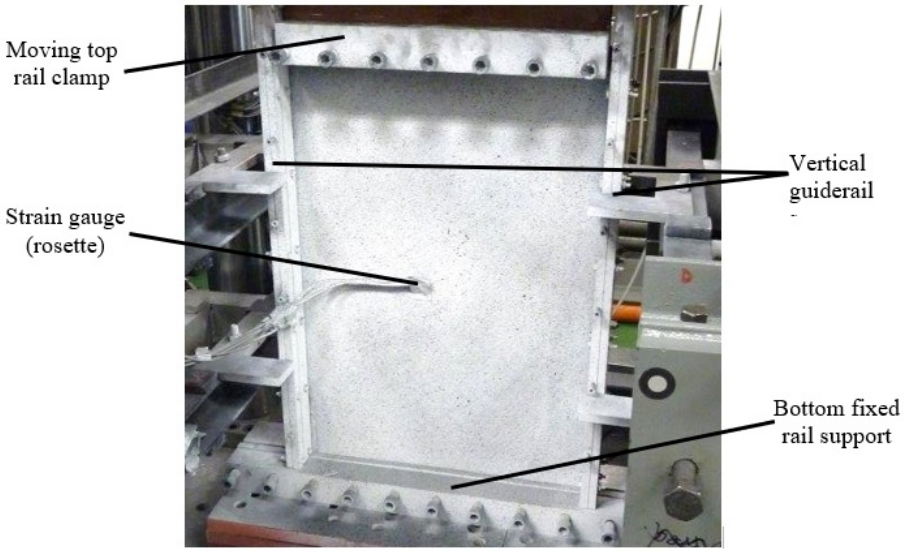


**Figure 14. Panel assembly in the MTS test frame.**

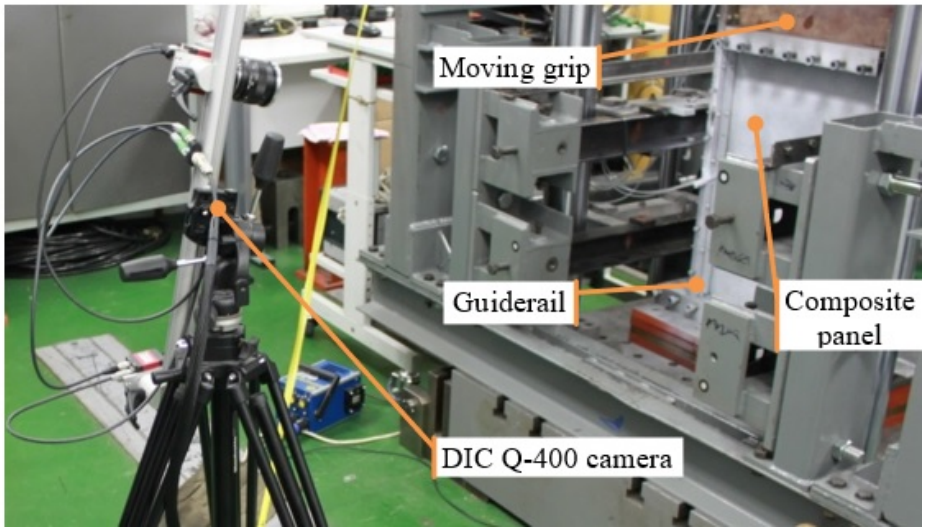


**Figure 15. Panel test configuration.**

## 4.2. Experimental results and evaluation

Each panel was subjected to axial compressive loading up to 125 kN and subsequently unloaded to zero load. The loading rate was fixed to 1 mm/min. Figures 16 to 20 show the strains measured using the back-to-back (side A and side B) rosette strain gauges for each panel. Strain gauges labeled 2 and 5 were placed in the axial compressive force direction. The strain vs. load graphs up to maximum applied force are shown. At the maximum load levels the buckling mode was fully developed for all panels.

Table 1 shows the overview of the buckling load for the different panels. For each alternative, two panels were tested. The mean values and the difference between both test are shown in Table 1. Figures 21 and 22 present the DIC out-of-plane displacement optically at 120 kN. Although the predicted onset of buckling mode of the reference CS panels was nearly the same, the actual buckling load of CYTEC TX1100/PRISM EP2400 system was 8.6% higher compared to the predicted value and by about 16.9% compared to the same benchmark made out of of the HiTape/RTM system.

The same buckling load was measured for the variable stiffness, variable thickness panel , with HiTape/RTM system, as the variable thickness panel, with TX1100/PRISM EP2400 system. While the maximum out-of-plane deformation of HiTape/RTM alternatives at 120 kN was observed between $\pm$ 5 to 6 mm, TX1100/PRISM EP2400 alternatives showed only $\pm$ 2 to 4 mm out-of-plane deformation. The smallest out-of-plane displacement was observed for the benchmark with 26 layers (TX1100/PRISM EP2400 system). This panel also displayed a different buckling mode compared to all other panels. While the VS and benchmark with 40 layers showed two buckling half-waves, the VS and VSVT showed three buckling half-waves, and the benchmark with 40 layers buckled with only one half-wave. It should be noted that the initiation of the buckling mode and its subsequent development evaluation based on strain gauge measurements can be slightly affected by strain gauges' location. Due to different buckling modes in combination with strain gauge placing as can be seen in Figures 21 and 22 (the strain gauge locations are labeled by black rectangles), the buckling mode development cannot always be captured accurately.

**Table 1. Overview of the buckling load.**

| panel [–] | predicted buckling load [kN] | average buckling load [kN] | difference between two panels [kN] | deviation from prediction [%] | deviation from benchmark [%] |
|---|---|---|---|---|---|
| benchmark, 26 layers | 71.8 | 78.0 | 4.0 | 8.6 | - |
| VT | 85.2 | 75.5 | 3.0 | -11.4 | -3.2 |
| benchmark, 40 layers | 71.1 | 68.5 | 7.0 | -3.7 | - |
| VS | 60.2 | 63.5 | 3.0 | 5.5 | -7.3 |
| VSVT | 73.3 | 76.5 | 3.0 | 4.4 | 11.7 |

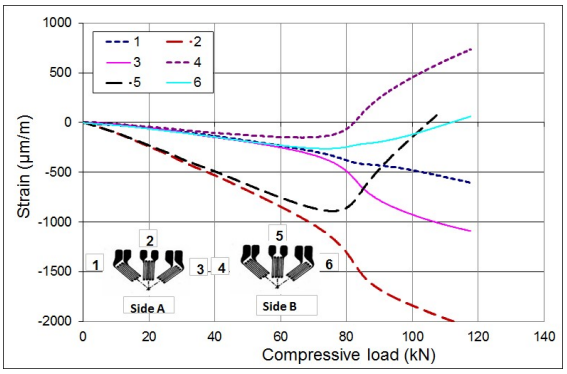


**Figure 16. Strain measurements against applied load for the variable stiffness panel.**

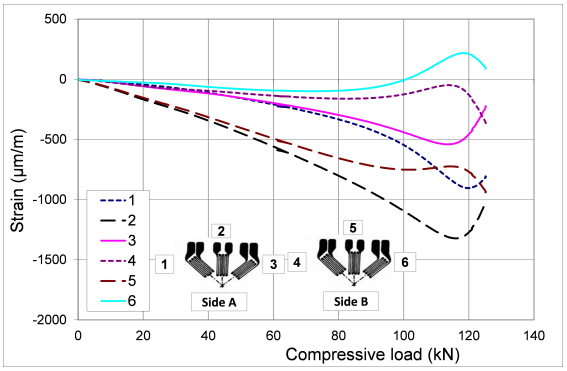


**Figure 17. Strain measurements against applied load for 40-layer benchmark.**

# 5. Discussion

When observing the test results, it is noticed that they correlate quite well with the predictions: only one case is more than 10% off. The difference between panels of the same lay-up is small

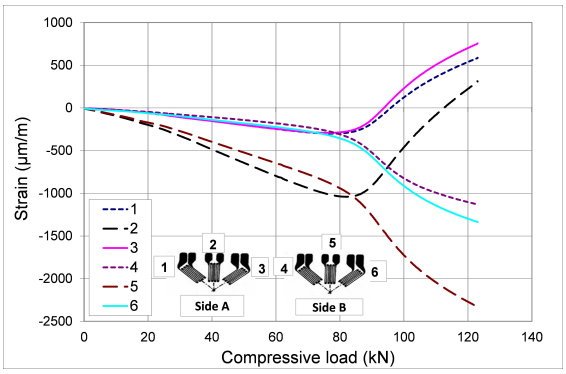


**Figure 18. Strain measurements against applied load for variable stiffness variable thickness.**

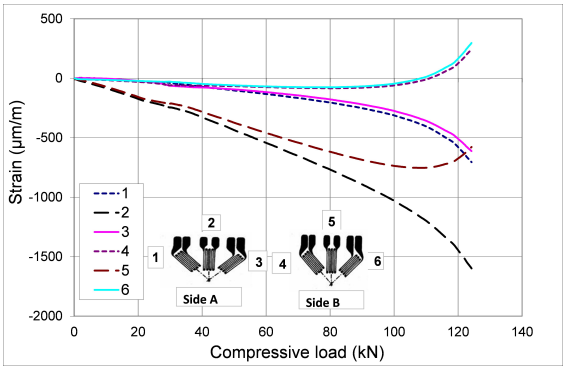


**Figure 19. Strain measurements against applied load for 26-layer benchmark.**

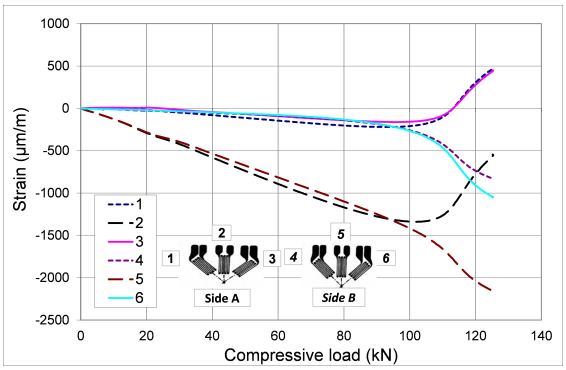


**Figure 20. Strain measurements against applied load for variable thickness.**

as well: only in the case of the benchmark with 40 layers, the difference between both panels is more than 5% of the buckling load. This indicates that the manufacturing and testing have been performed twice in the same way and the results are reliable.

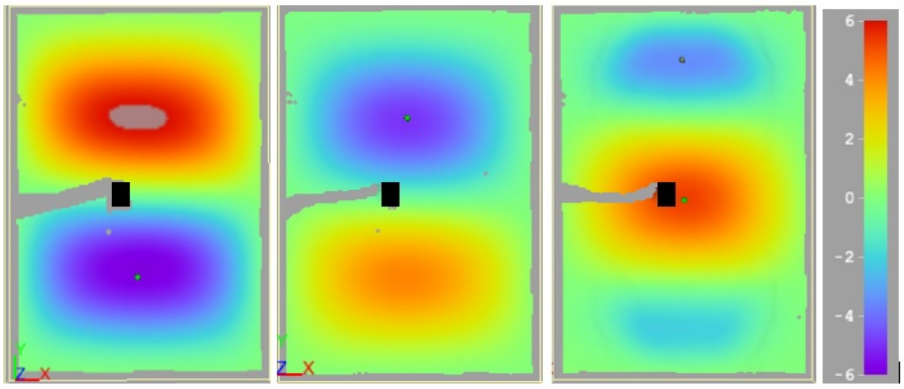


**Figure 21. Comparison of out-of-plane displacement using DIC full-field measurement at 120 kN (variable stiffness - left, 40-layer benchmark middle, variable thickness right) (black rectangles indicate the location of the strain gauges).**

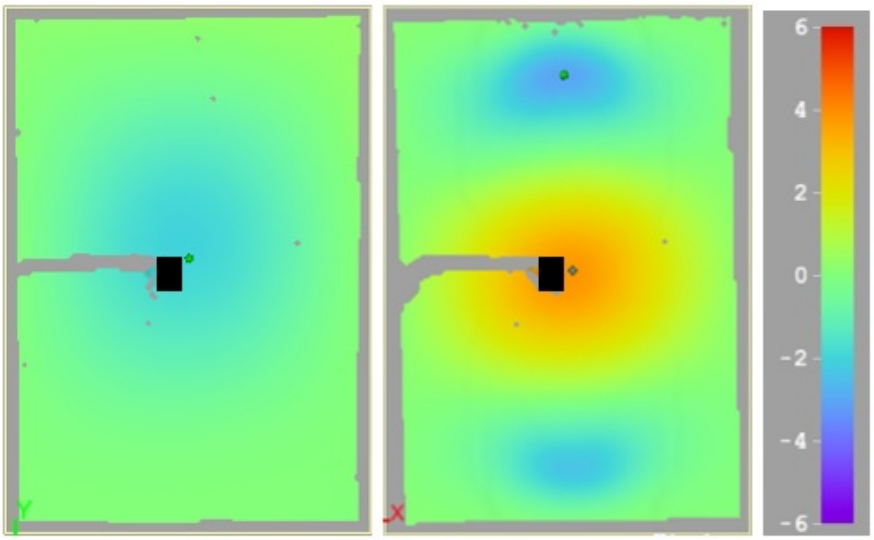


**Figure 22. Comparison of out-of-plane displacement using DIC full-field measurement at 120 kN (26-layer benchmark - left, variable thickness right) (black rectangles indicate the location of the strain gauges).**

Before going into detail about the different cases, it should be noted that buckling load scales with the thickness cubed. This means that by saving 15% of weight, the buckling load goes down by 38.5%. When the buckling loads found are normalized this way, a substantial increase is found for each case. This highlights the advantage of fiber steering or varying the thickness over a

structure.

When looking in more detail to the results obtained using the TX1100 material, the benchmark case fits fairly well. For the variable stiffness case, the buckling load is over-predicted. Three reasons contribute to this effect. One, the actual lay-out that has been found after optimization is slightly changed during manufacturing: no minimum distance between ply drops or minimum size of the patches is taken into account during optimization. Two, the resin-rich areas which appear at ply drop locations are not taken into account in the finite element analysis: this are weak points in the structure and can act as imperfections. Three, the neutral axis is not a straight line as has been assumed during analysis, but is varying with thickness since the laminate is built up from one side: this means that some extra load may appear due to the changing position of the axis.

When looking at the results with the HiTape material, it stands out that the benchmark performs less good than the benchmark with the other material. Theoretically they have to have almost the same buckling load, but in reality there is a 9.5 kN difference in buckling load. The benchmark with the TX1100 material performed slightly better than expected, while the HiTape material performs a bit less. This could also be due to the material properties varying a bit, for example the value of $E_{11}$ used, which can be slightly different in compression, than in tension, which value was used in the current work. For a fair comparison, the plates that are 15% lighter are compared to the benchmark of the same material.

The variable stiffness plate performs a bit better than expected, but not as good as the benchmark: the radii that can be achieved in this case are not tight enough to increase the buckling load enough. When normalizing the load with respect to the weight, a 40% improvement is found, which is significant. The slightly higher buckling load than expected can be explained by the thermal stresses that occur during curing [76, 77]: these introduce a bit of pre-stress into the plate which is advantageous for buckling. On the other hand, during manufacturing gaps and overlaps are created which are not taken into account during the analysis. In the end it turns out that for this specific example the positive effect of the pre-stress outweighs the negative effect of the the gaps and overlaps.

The variable stiffness variable thickness laminate not only performed a bit better than expected, but also outperformed the benchmark. The reasons for the analysis not being completely spot on

are a combination of what was said for the variable stiffness and variable thickness: on one hand the resin rich areas, gaps and overlaps have a negative effect, the thermal pre-stress has a positive effect. In the end all these effects seem to be almost canceling each other out. This shows that 15% weight saving is possible by using a combination of fiber steering and dropping plies.

# 6. Conclusion

In the current work, rectangular panels of $400 \times 600$ mm were optimized, manufactured and tested in compression until buckling. Four types of panels were built using dry fiber placement in vacuum-assisted resin infusion: a benchmark case only consisting of $0°$, $\pm 45°$, and $90°$, a variable stiffness case (steering fibers, constant number of layers), a variable thickness case (no fiber steering, internal ply drops), and a variable stiffness variable thickness case (fiber steering and internal ply drops). Compared to the benchmark, the other three cases were 15% lighter to highlight the possible weight improvements by moving away from the traditional fiber angles.

The optimization showed that only steering the fibers is not sufficient to obtain the same buckling load as the benchmark, although the improvement is still significant. Using fiber steering and variable thickness it was shown to be possible to match the buckling load, even with 15% weight saving. After optimization, some slight changes were necessary to obtain designs that were ready to manufacture. All panels were manufactured and tested successfully, with good repeatability between the different panels of the same type.

The test results were in reasonable agreement with numerical predictions. The variable stiffness panels buckled at a slightly higher than expected load. However, it was not enough to match the benchmark: the buckling load was 7.4% lower. Nonetheless, it should be emphasized that by saving 15% of weight a 38.5% decrease in buckling load is expected since buckling load scales with the thickness cubed. The increase in load compared to the prediction is most likely due to the thermal pre-stress in VS the panels due to curing. The variable thickness panel buckled at a lower load than expected, and also 3.2% lower than the benchmark. The lower than expected load is most likely due to the effect of the resin rich pockets at the ply drops, which is not taken into account in the simulations. The variable stiffness variable thickness panel performed better than

expected, and even 11.7% better than the benchmark. Again, the thermal pre-stress due to curing is probably the cause of the higher than expected buckling load.

Overall, the tests show that 15% weight saving is possible with the current design methods without reducing the buckling load. These results highlight the possibilities offered for lightweight structural design by non-conventional laminates over classical laminates made using only traditional fiber angles. Future work includes checking whether the conclusion also holds for more complicated structures, different load cases, and different structural responses.

# 7. Data availability

The raw/processed data required to reproduce these findings cannot be shared at this time due to legal or ethical reasons.

# 8. Acknowledgements

This work is supported by the CANAL (CreAting Non-conventionAl Laminates) project, part of the European Union Seventh Framework Program.

# References

[1] Lopes, C., Gürdal, Z., and Camanho, P., "Tailoring for strength of composite steered-fibre panels with cutouts," *Composites Part A: Applied Science and Manufacturing*, Vol. 41, No. 12, 2010, pp. 1760 – 1767.

[2] Gürdal, Z., Tatting, B., and Wu, C., "Variable stiffness composite panels: Effects of stiffness variation on the in-plane and buckling response," *Composites Part A: Applied Science and Manufacturing*, Vol. 39, No. 5, 2008, pp. 911 – 922.

[3] Hyer, M. W. and Charette, R. F., "Use of curvilinear fiber format in composite structure design," *AIAA Journal*, Vol. 29, No. 6, 2014/12/01 1991, pp. 1011–1015.

[4] van Campen, J. M., Kassapoglou, C., and Gürdal, Z., "Generating realistic laminate fiber angle distributions for optimal variable stiffness laminates," *Composites Part B: Engineering*, Vol. 43, No. 2, 2012, pp. 354 – 360.

[5] Stodieck, O., Cooper, J., Weaver, P., and Kealy, P., "Improved aeroelastic tailoring using tow-steered composites," *Composite Structures*, Vol. 106, 2013, pp. 703–715, cited By 7.

[6] Ungwattanapanit, T. and Baier, H., "Postbuckling analysis and optimization of stiffened fuselage panels utilizing variable-stiffness laminates," *Congress of the International Council of the Aeronautical Sciences, ICAS [29., 2014, St. Petersburg]*, 2014.

[7] Liu, W. and Butler, R., "Buckling optimization for composite panels with elastic tailoring," *49th AIAA/ASME/ASCE/AHS/ASC Structures, Structural Dynamics and Materials Conference*, April 2008.

[8] Coburn, B., Wu, Z., and Weaver, P., "Buckling analysis of stiffened variable angle tow panels," *Composite structures*, Vol. 111, No. 1, 2014, pp. 259–270.

[9] Wu, Z., Weaver, P. M., Raju, G., and Kim, B. C., "Buckling analysis and optimisation of variable angle tow composite plates," *Thin-Walled Structures*, Vol. 60, No. 0, 2012, pp. 163 – 172.

[10] Wu, Z., Weaver, P., and Raju, G., "Postbuckling optimisation of variable angle tow composite plates," *Composite structures*, Vol. 103, 2013, pp. 34–42.

[11] Guimaraes, T., Castro, S., Rade, D., and Cesnik, C., "Panel Flutter Analysis and Optimization of Composite Tow Steered Plates," *58th AIAA/ASMe/ASCE/AHS/SC Structures, Structural Dynamics, and Materials Conference*, 2017.

[12] Alhajahmad, A., Abdalla, M., and Z., G., "Design Tailoring for Pressure Pillowing Using Tow-Placed Steered Fibers," *Journal of aircraft*, Vol. 45, 2008, pp. 630–640.

[13] Demasi, L., Santarpia, E., R, C., Biagini, G., and Vannucci, F., "Zig-Zag and Layer wise theories for Variable-Stiffness composite laminates based on the Generalized Unified Formulation," *58th AIAA/ASMe/ASCE/AHS/SC Structures, Structural Dynamics, and Materials Conference*, 2017.

[14] Dems, K. and Winiewski, J., "Optimal design of fibre-reinforced composite disks," *Journal of theoretical and applied mechanics*, Vol. 47, 2009, pp. 515–535.

[15] Parnas, L., Oral, S., and Ceyhan, U., "Optimum design of composite structures with curved fiber courses," *Composite science and technology*, Vol. 63, 2003, pp. 1071–1082.

[16] Kim, B., Potter, K., and Weaver, P., "Continuous tow shearing for manufacturing variable angle tow composites," *Composites, Part A: Applied Science and Manufacturing*, Vol. 43, No. 8, 2012, pp. 1347–1356.

[17] Honda, S. and Narita, Y., "Natural frequencies and vibration modes of laminated composite plates reinforced with arbitrary curvilinear fiber shape paths," *Journal of sound and vibrations*, Vol. 331, 2012, pp. 180–191.

[18] Honda, S., Narita, Y., and Sasaki, K., "Maximizing the Fundamental Frequency of Laminated Composite Plates with Optimally Shaped Curvilinear Fibers," *Journal of system design and dynamics*, Vol. 3, 2009, pp. 867–876.

[19] Montemurro, M. and Catapano, A., "On the effective integration of manufacturability constraints within the multi-scale methodology for designing variable angle-tow laminates," *composite structures*, Vol. 161, 2017, pp. 145–159.

[20] Nagendra, S., Kodiyalam, S., Davis, J. E., and Parthasarathy, V. N., "Optimization of Tow Fiber Paths for Composite Design," *36th AIAA/American Society of Mechanical Engineers/American Society of Civil Engi-*

*neers/American Helicopter Society/ Society for Composites Structures, Structural Dynamics, and Materials Conference*, 1995.

[21] Wu, K., Tatting, B., Smith, B., Stevens, R., Occhipinti, G., and Swift, J., "Design and manufacturing of tow-steered composite shells using fiber placement," *50th AIAA/ASMe/ASCE/AHS/SC Structures, Structural Dynamics, and Materials Conference*, 2009.

[22] Fayazbakhsh, K., Nik, M., Pasini, D., and Lessard, L., "Defect layer method to capture effect of gaps and overlaps in variable stiffness laminates made by Automated Fiber Placement," *Composite Structures*, Vol. 97, 2013, pp. 245 – 251.

[23] Blom, A., Stickler, P., and Gürdal, Z., "Optimization of a composite cylinder under bending by tailoring stiffness properties in circumferential direction," *composites part B Engineering*, Vol. 41, 2010, pp. 157–165.

[24] Nik, M., Fayazbakhsh, K., Pasini, D., and Lessard, L., "Optimization of variable stiffness composites with embedded defects induced by Automated Fiber Placement," *Composite Structures*, Vol. 107, 2014, pp. 160 – 166.

[25] Akbarzadeh, A., Arian Nik, M., and Pasini, D., "The role of shear deformation in laminated plates with curvilinear fiber paths and embedded defects," *composite structures*, Vol. 118, 2014, pp. 217–227.

[26] van den Brink WM, Vankan, W., and Maas, R., "Buckling optimized variable stiffness laminates for a composite fuselage window section," *28th international congress of the aeronautical sciences*, 2012.

[27] Gürdal, Z., Tatting, B., and Wu, K., "Tow-Placement Technology and Fabrication Issues for Laminated Composite Structures," *46th AIAA/ASME/ASCE/AHS/ASC Structures, Structural Dynamics and Materials Conference*, American Institute of Aeronautics and Astronautics, 2014/11/30 2005.

[28] Tatting, B. F., Gürdal, Z., and Jegley, D., "Design and manufacture of elastically tailored tow placed plates," 2002.

[29] Crothers, P., Drechsler, K., Feltin, D., Herszberg, I., and Kruckenberg, T., "Tailored fibre placement to minimise stress concentrations," *Composites Part A: Applied Science and Manufacturing*, Vol. 28, No. 7, 1997, pp. 619 – 625.

[30] Richter, E., Uhlig, K., Spickenheuer, A., Bittrich, L., Maäder, E., and Heinrich, G., "thermoplastic composite parts based on online spun commingled hybrid yarns with continuous curvilinear fibre patterns," *16th European Conference on Composite Materials*, June 2014.

[31] Tosh, M. and Kelly, D., "On the design, manufacture and testing of trajectorial fibre steering for carbon fibre composite laminates," *Composites Part A: Applied Science and Manufacturing*, Vol. 31, No. 10, 2000, pp. 1047 – 1060.

[32] Kim, B., Potter, K., and Weaver, P., *Multi-tow shearing mechanism for high-speed manufacturing of variable angle tow composites*, 2012, Venice, IT.

[33] Groh, R. and Weaver, P., "Mass Optimization of Variable Angle Tow, Variable Thickness Panels with Static

Failure and Buckling Constraints," *56th AIAA/ASME/ASCE/AHS/ASC Structures, Structural Dynamics and Materials Conference*, January 2015.

[34] Liu, W. and Butler, R., "Buckling Optimization of Variable-Angle-Tow Panels Using the Infinite-Strip Method," *AIAA Journal*, Vol. 51, No. 6, 2015/01/29 2013, pp. 1442–1449.

[35] Ghiasi, H., Fayazbakhsh, K., Pasini, D., and Lessard, L., "Optimum stacking sequence design of composite materials Part II: Variable stiffness design," *Composite Structures*, Vol. 93, No. 1, 2010, pp. 1 – 13.

[36] IJsselmuiden, S. T., *Optimal design of variable stffness composite structures using lamination parameters*, Ph.D. thesis, Delft University of Technology, 2011.

[37] Peeters, D., van Baalen, D., and Abdalla, M., "Combining topology and lamination parameter optimisation," *Structural and Multidisciplinary Optimization*, 2015, pp. 1–16.

[38] Autio, M., "Determining the real lay-up of a laminate corresponding to optimal lamination parameters by genetic search," *Structural and Multidisciplinary Optimization*, Vol. 20, No. 4, 2000, pp. 301–310.

[39] Setoodeh, S., Blom, A., Abdalla, M., and Gürdal, Z., "Generating Curvilinear Fiber Paths from Lamination Parameters Distribution," *47th AIAA/ASME/ASCE/AHS/ASC Structures, Structural Dynamics, and Materials Conference*, American Institute of Aeronautics and Astronautics, 2014/12/01 2006.

[40] van Campen, J. and Gürdal, Z., "Retrieving Variable Stiffness Laminates from Lamination Parameters Distribution," *50th AIAA/ASME/ASCE/AHS/ASC Structures, Structural Dynamics, and Materials Conference*, American Institute of Aeronautics and Astronautics, 2014/12/01 2009.

[41] Blom, A. W., Abdalla, M. M., and Gürdal, Z., "Optimization of course locations in fiber-placed panels for general fiber angle distributions," *Composites Science and Technology*, Vol. 70, No. 4, 2010, pp. 564 – 570.

[42] Jung-Seok Kim, C.-G. K. and Hong, C.-S., "Optimum design of composite structures with ply drop using genetic algorithm and expert system shell," *Composite Structures*, Vol. 46, No. 2, 1999, pp. 171 – 187.

[43] Adams, D. B., Watson, L. T., Gürdal, Z., and Anderson-Cook, C. M., "Genetic algorithm optimization and blending of composite laminates by locally reducing laminate thickness," *Advances in Engineering Software*, Vol. 35, No. 1, 2004, pp. 35 – 43.

[44] IJsselmuiden, S. T., Abdalla, M. M., Seresta, O., and Gürdal, Z., "Multi-step blended stacking sequence design of panel assemblies with buckling constraints," *Composites Part B: Engineering*, Vol. 40, No. 4, 2009, pp. 329 – 336.

[45] Sørensen, S. and Stolpe, M., "Global blending optimization of laminated composites with discrete material candidate selection and thickness variation," *Structural and Multidisciplinary Optimization*, 2015, pp. 1–19.

[46] Liu, D., Toroporov, V. V., Querin, O. M., and Barton, D. C., "Bilevel Optimization of Blended Composite Wing Panels," *Journal of Aircraft*, Vol. 48, No. 1, 2015/07/01 2011, pp. 107–118.

[47] De Leon, D., de Souza, C., Fonseca, J., and da Silva, R., "Aeroelastic tailoring using fiber orientation and topology optimization," *Structural and Multidisciplinary Optimization*, Vol. 46, No. 5, 2012, pp. 663–677.

[48] Delgado, G., *Optimization of composite structures: A shape and topology sensitivity analysis*, Theses, Ecole Polytechnique X, June 2014.

[49] Sørensen, S. N., Sørensen, R., and Lund, E., "DMTO a method for Discrete Material and Thickness Optimization of laminated composite structures," *Structural and Multidisciplinary Optimization*, Vol. 50, No. 1, 2014, pp. 25–47.

[50] Lund, E., "Buckling topology optimization of laminated multi-material composite shell structures," *Composite Structures*, Vol. 91, No. 2, 2009, pp. 158 – 167.

[51] Srensen, R. and Lund, E., "Thickness filters for gradient based multi-material and thickness optimization of laminated composite structures," *Structural and Multidisciplinary Optimization*, 2015, pp. 1–24.

[52] Joshi, M. G. and Jr, S. B. B., "Thickness optimization for maximum buckling loads in composite laminated plates," *Composites Part B: Engineering*, Vol. 27, No. 2, 1996, pp. 105 – 114.

[53] Irisarri, F.-X., Lasseigne, A., Leroy, F.-H., and Riche, R. L., "Optimal design of laminated composite structures with ply drops using stacking sequence tables," *Composite Structures*, Vol. 107, No. 0, 2014, pp. 559 – 569.

[54] Hyer, M. W., Rust, R., and Waters Jr., W., "Innovative design of composite structures: design. manufacturing and testing of plates utilizing curvilinear fiber trajectories." *NASA Contractor Report 197045*, 1994.

[55] Hyer, M. and Lee, H., "The use of curvilinear fiber format to improve buckling resistance of composite plates with central circular holes," *Composite Structures*, Vol. 18, No. 3, 1991, pp. 239 – 261.

[56] Jegley, D. C., Tatting, B. F., and Gürdal, Z., "Optimization of elastically tailored tow-placed plates with holes," *Proceedings of the AIAA/ASME/ASCE/AHS/ASC 44th Structures, Structural Dynamics and Materials Conference, Norfolk, VA*, 2003, pp. 2003–1420.

[57] Jegley, D., Tatting, B., and Gürdal, Z., "Tow-steered panels with holes subjected to compression or shear loading," *Proceedings of the AIAA/ASME/ASCE/AHS/ASC 46th structures, structural dynamics and materials (SDM) conference, Austin, TX*, 2005, pp. 2005–2017.

[58] Blom, A., *Strucural Performance of Fibre-Placed Variable-Stiffness Composite Conical and Cylindrical Shells*, Ph.D. thesis, Delft University of Technology, 2010.

[59] Wu, C., "Design and Analysis of Tow-Steered Composite Shells Using Fiber Placement," *Proceedings of the ASC 23rd Annual Technical Conference, Memphis, Tennessee, September 9-11, 2008, paper no. 125.*, 2008.

[60] Wu, C., Tatting, B., Smith, B., Stevens, R., Occhipinti, G., Swift, J., D.Achary, and Thornburgh, R., "Design and Manufacturing of Tow-Steered Composite Shells Using Fiber Placement," *Proceedings of the 50th AIAA/ASME/ASCE/AHS/ASC Structures, Structural Dynamics, and Materials Conference*, 2009.

[61] Wu, C., Stanford, B., Hrinda, G., Wang, Z., Martin, R., and Kim, H., "Structural Assessment of Advanced Tow-Steered Shells," *Proceedings of the 54th AIAA/ASME/ASCE/AHS/ASC Structures, Structural Dynamics, and Materials Conference*, 2013.

[62] Wu, C., Stanford, B., Turpin, J., and Martin, R., "Structural Performance of Advanced Composite Tow-Steered

Shells With Cutouts," *Proceedings of the 55th AIAA/ASME/ASCE/AHS/ASC Structures, Structural Dynamics, and Materials Conference*, 2014.

[63] Wu, C., Turpin, J., Gardner, N., Stanford, B., and Martin, R., "Structural Characterization of Advanced Composite Tow-Steered Shells with Large Cutouts," *Proceedings of the 56th AIAA/ASME/ASCE/AHS/ASC Structures, Structural Dynamics, and Materials Conference*, 2015.

[64] Wu, C., Farrokh, B., Stanford, B., and Weaver, P., "Imperfection Insensitivity Analyses of Advanced Composite Tow-Steered Shells," *Proceedings of the 57th AIAA/ASME/ASCE/AHS/ASC Structures, Structural Dynamics, and Materials Conference*, 2016.

[65] Zucco, G., Oliveri, V., Peeters, D., Telford, R., Clancy, G., McHale, C., Rouhi, M., O'Higgins, R., Young, T. M., and Weaver, P. M., "Static Test of a Thermoplastic Composite Wingbox Under Shear and Bending Moment," *SciTech Conference, 8 to 12 January 2018 Gaylord Palms, Kissimmee, Florida*, 2018.

[66] Oliveri, V., Peeters, D., Clancy, G., O'Higgins, R., Jones, D., and Weaver, P. M., "Design, optimization and manufacturing of a unitized thermoplastic wing-box structure," *SciTech Conference, 8 to 12 January 2018 Gaylord Palms, Kissimmee, Florida*, 2018.

[67] Irisarri, F.-X., Peeters, D., and Abdalla, M., "Optimisation of ply drop order in variable stiffness laminates," *Composite Structures*, Vol. 152, 2016, pp. 791–799.

[68] Peeters, D. and Abdalla, M., "Optimisation of Variable Stiffness Composites with Ply Drops," *56th AIAA/ASCE/AHS/ASC Structures, Structural Dynamics, and Materials Conference*, American Institute of Aeronautics and Astronautics, July 2015.

[69] Peeters, D., Hesse, S., and Abdalla, M., "Stacking sequence optimisation of variable stiffness laminates with manufacturing constraints," *Composite Structures*, Vol. 125, 2015, pp. 596 – 604.

[70] Irisarri, F.-X., Lasseigne, A., Leroy, F.-H., and Riche, R. L., "Optimal design of laminated composite structures with ply drops using stacking sequence tables," *Composite Structures*, Vol. 107, No. 0, 2014, pp. 559 – 569.

[71] Abdalla, M. M., Kassapoglou, C., and Gürdal, Z., "Formulation of composite laminate robustness constraint in lamination parameters space," *Proceedings of 50th AIAA/ASME/ASCE/AHS/ASC structures, structural dynamics, and materials conference. Palm Springs, California*, 2009.

[72] "FlexTest 40 control system manual, DS2.42684 311 Dynamic High Force System, MTS System Corporation, June 23, 2011," .

[73] "BMCM module system user manual for PCI-Base (PCI-Base500/300, MAD/MDA, MVLxx), BMC Messysteme GmbH, 2010." .

[74] "NextView4 User Manual Version 4.5, BMC Messysteme GmbH, 2011, p.232." .

[75] "ISTRA 4D User Manual Version 4.3, Dantec Dynamics GmbH, 2011, p.66." .

[76] Lopes, C., Camanho, P., Gürdal, Z., and Tatting, B., "Progressive failure analysis of tow-placed, variable-stiffness composite panels," *International Journal of Solids and Structures*, Vol. 44, No. 25, 2007, pp. 8493 –

8516.

[77] Abdalla, M. M., Gürdal, Z., and Abdelal, G. F., "Thermomechanical Response of Variable Stiffness Composite Panels," *Journal of Thermal Stresses*, Vol. 32, No. 1-2, 2008, pp. 187–208.